

OPEN

# Facile synthesis of hydrophilic magnetic graphene nanocomposites via dopamine self-polymerization and Michael addition for selective enrichment of N-linked glycopeptides

Changfen Bi<sup>1</sup>, Ye Yuan<sup>1</sup>, Yuran Tu<sup>2</sup>, Jiahui Wu<sup>2</sup>, Yulu Liang<sup>2</sup>, Yiliang Li<sup>1,\*</sup>, Xiwen He<sup>2</sup>, Langxing Chen<sup>2,3\*</sup> & Yukui Zhang<sup>4</sup>

The development of methods to effectively capture N-glycopeptides from the complex biological samples is crucial to N-glycoproteome profiling. Herein, the hydrophilic chitosan-functionalized magnetic graphene nanocomposites (denoted as Fe<sub>3</sub>O<sub>4</sub>-GO@PDA-Chitosan) were designed and synthesized via a simple two-step modification (dopamine self-polymerization and Michael addition). The Fe<sub>3</sub>O<sub>4</sub>-GO@PDA-Chitosan nanocomposites exhibited good performances with low detection limit (0.4 fmol·μL<sup>-1</sup>), good selectivity (mixture of bovine serum albumin and horseradish peroxidase tryptic digests at a molar ration of 10:1), good repeatability (4 times), high binding capacity (75 mg·g<sup>-1</sup>). Moreover, Fe<sub>3</sub>O<sub>4</sub>-GO@PDA-Chitosan nanocomposites were further utilized to selectively enrich glycopeptides from human renal mesangial cell (HRMC, 200 μg) tryptic digest, and 393 N-linked glycopeptides, representing 195 different glycoproteins and 458 glycosylation sites were identified. This study provides a feasible strategy for the surface functionalized novel materials for isolation and enrichment of N-glycopeptides.

Protein N-glycosylation, as one of the most prevalent post-translational modifications (PTMs), can significantly change the structure, increase stability and subsequently endow new functions of protein<sup>1-3</sup>. Meanwhile, this modification plays determinant roles in physiological processes, such as molecular and cell recognition, signal transduction, immune response. Aberrant protein N-glycosylation is associated with human disease, such as rheumatoid arthritis, lupus erythematosus, Alzheimer's disease (AD) and so on<sup>4-6</sup>. Therefore, the thorough analysis of protein N-glycosylation is beneficial for elucidating pathogenesis of many diseases and for the discovery of new clinical biomarkers and effective disease control<sup>7</sup>. In the recent years, mass spectrometry (MS) has been widely used in N-glycoproteome analysis due to its high sensitivity and high-throughput and capacity to analyze disease-associated glycoforms<sup>8</sup>. However, the low abundance of N-glycoproteins in biological samples, poor ionization of N-glycopeptides and the heterogeneity of glycan structures make the direct MS analysis extremely difficult<sup>8</sup>. Therefore, an enrichment step of N-glycopeptides prior to MS analysis is a prerequisite for the successful glycoproteomics analysis.

A variety of enrichment strategies towards glycoproteins/glycopeptides have been developed, such as boronic acid chemistry<sup>9-12</sup>, immobilized metal ion affinity chromatography (IMAC)<sup>13-15</sup>, molecularly imprinting

<sup>1</sup>Tianjin Key Laboratory of Radiation Medicine and Molecular Nuclear Medicine, Institute of Radiation Medicine, Peking Union Medical College & Chinese Academy of Medical Sciences, Tianjin, 300192, China. <sup>2</sup>College of Chemistry, Tianjin Key Laboratory of Biosensing and Molecular Recognition, State Key Laboratory of Medicinal Chemical Biology, Nankai University, Tianjin, 300071, China. <sup>3</sup>Collaborative Innovation Center of Chemical Science and Engineering (Tianjin), Tianjin, 300071, China. <sup>4</sup>Dalian Institute of Chemical Physics, Chinese Academy of Sciences, Dalian, 116023, China. \*email: [liyiliang75@163.com](mailto:liyiliang75@163.com); [lxchen@nankai.edu.cn](mailto:lxchen@nankai.edu.cn)

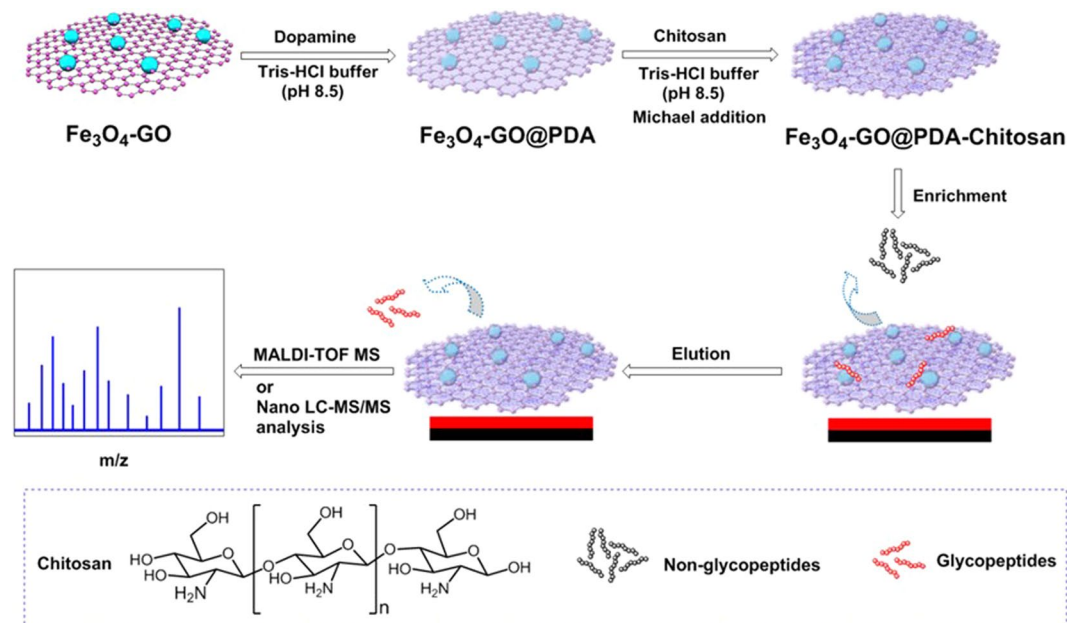


**Figure 1.** Schematic illustration of the procedure for preparation of  $\text{Fe}_3\text{O}_4\text{-GO@PDA}$  and  $\text{Fe}_3\text{O}_4\text{-GO@PDA-Chitosan}$  and N-glycopeptides enrichment.

method<sup>16–18</sup>, hydrophilic interaction liquid chromatography (HILIC)<sup>19–21</sup> and so on. Among them, owing to good MS compatibility, excellent reproducibility, unbiased enrichment performance and simple operating process, HILIC approach, based on the hydrophilicity differences between glycopeptides and non-glycopeptides, is widely adopted in glycopeptides enrichment. Chitosan is a cationic polymer obtained by deacetylation of chitin, and has gained more attention as drug delivery carriers owing to its bio-safety, biocompatibility and biodegradability<sup>22</sup>. The polar groups ( $-\text{OH}$ ,  $-\text{NH}_2$ ) endowed chitosan with selectivity towards glycopeptides through hydrogen bond between the glycan moieties and  $-\text{OH}/-\text{NH}_2$ . Chitosan microspheres as adsorbent for isolation need an inconvenient and time-consuming centrifugation separation<sup>23</sup>. In recent years, magnetic separation has received extensive attention because of its better separation efficiency in contrast to the traditional approach. The combination of HILIC enrichment strategy and magnetic separation technology realized the rapid and efficient enrichment and separation of glycoproteins/glycopeptides. Li *et al.* fabricated  $\text{Fe}_3\text{O}_4\text{@G6P}$  magnetic microspheres for specific capture of N-linked glycopeptides<sup>24</sup>. The hydrophilic glucose-6-phosphate immobilized on the  $\text{Fe}_3\text{O}_4$  nanoparticles endowed the microspheres with high selectivity and sensitivity. Fang *et al.* modified chitosan on magnetic  $\text{Fe}_3\text{O}_4$  nanoparticles<sup>25</sup>. The HILIC microspheres showed the strong ability of fast magnetic separation and recognition toward glycopeptides. Notwithstanding these excellent reports, the synthesis of novel magnetic materials is still attracting extensive attentions aimed at optimizing the enrichment selectivity and sensitivity towards glycoproteins/glycopeptides. Magnetic  $\text{Fe}_3\text{O}_4$  nanoparticle-decorated GO ( $\text{Fe}_3\text{O}_4\text{-GO}$ ) has magnetic responsibility and large surface area, and has been widely used for glycoproteins/glycopeptides enrichment<sup>26,27</sup>. Although some efficient strategies (self-assembly, Au-S bond) were applied to fabricate hydrophilic materials, they suffered from tedious operation<sup>28,29</sup>. Based on these, the assembly of chitosan coated  $\text{Fe}_3\text{O}_4\text{-GO}$  nanocomposites by a convenient Michael addition reaction would be very attractive.

Herein, a new type of chitosan-functionalized hydrophilic magnetic nanocomposites,  $\text{Fe}_3\text{O}_4\text{-GO@PDA-Chitosan}$  (Fig. 1) was assembled via dopamine self-polymerization and Michael addition. Briefly,  $\text{Fe}_3\text{O}_4$  NPs were interspersed on the surface of graphene oxide nanocomposites by solvothermal reaction. Polydopamine (PDA)-coated magnetic graphene was prepared via dopamine self-polymerization. Chitosan was grafted on the surface of  $\text{Fe}_3\text{O}_4\text{-GO@PDA}$  nanocomposites via Michael addition. The dopamine self-polymerization and Michael addition reaction occurred simply under mechanical agitation in Tris-HCl buffer. The polydopamine layer and chitosan on the surface of magnetic graphene could effectively enhance hydrophilic enrichment performance of magnetic nanocomposites for N-glycopeptides from the complex biological samples under an external magnetic field. This novel nanocomposite was applied to achieve good selectivity (mixture of bovine serum albumin and horseradish tryptic digests at a molar ration of 10:1), sensitivity ( $0.4 \text{ fmol}\cdot\mu\text{L}^{-1}$ ), binding capacity ( $75 \text{ mg}\cdot\text{g}^{-1}$ ) for N-glycopeptides enrichment.

## Experimental Section

**Materials.** Chitosan (with a deacetylation, degree of 98%) was purchased from Aladdin (Shanghai, China). Horseradish peroxidase (HRP), immunoglobulin G (IgG), peptide-N4-(N-acetyl- $\beta$ -D-glucosaminyl) asparagine amide F (PNGase F), bovine serum albumin (BSA), and HPLC-grade acetonitrile (ACN) were purchased from Sigma-Aldrich (USA) (Beijing, China). Dithiothreitol (DTT), urea, ammonium bicarbonate ( $\text{NH}_4\text{HCO}_3$ ) and iodoacetamide (IAA) were obtained purchased from Solarbio (China). Trifluoroacetic acid (TFA) was purchased

from J&K (Beijing, China). 2,5-Dihydroxybenzoic acid (DHB) was obtained from TCI (Japan) (Shanghai, China). Trypsin was from Sangon Biotech Co. Ltd. (Shanghai, China). Graphene oxide (GO) was purchased from XF NANO (Nanjing, China). Dopamine chloride and tris(hydroxymethyl)aminomethane (Tris) were obtained from Tianjin Heowns Biotech Co. Ltd. (Tianjin, China). Iron (III) chloride hexahydrate ( $\text{FeCl}_3 \cdot 6\text{H}_2\text{O}$ ), sodium acetate (NaAc), ethylene glycol (EG), acetic acid, hydrogen peroxide ( $\text{H}_2\text{O}_2$ ), ethanol, methanol were purchased from Concord Chemical Ltd. (Tianjin, China). Deionized water (18.25 M $\Omega$  cm) was prepared with a Milli-Q water purification system (Millipore, Milford, MA, USA).

**Characterization.** The morphology, structure and performance of the synthesized nanocomposites were evaluated according to a previous report<sup>30</sup>. Transmission electron microscope (TEM) images were obtained on a JEM-2100F (Japan) transmission electron microscope. Fourier transform infrared (FT-IR) spectra (4000–400  $\text{cm}^{-1}$ ) in KBr were recorded using the BRUKER TENSOR 27 Fourier transform infrared spectrophotometer. The crystal structure of the nanocomposites was performed on a Rigaku (Japan) D/max/2500 v/pc with nickel-filtered  $\text{Cu K}\alpha$  source. The XRD patterns were collected in the range  $3 < 2\theta < 80^\circ$  at a scan rate of  $4.0^\circ/\text{min}$ . The X-ray photoelectron spectra were obtained on a Thermo Fischer (USA) ESCALAB 250Xi X-ray photoelectron spectrometer (XPS) with an  $\text{Mg K}\alpha$  anode (15 kV, 400 W) at a takeoff angle of  $45^\circ$ . The source X-rays were not filtered and the instrument was calibrated against the C 1s band at 285 eV. The magnetic properties were analyzed with a LDJ9600-1 (USA) vibrating sample magnetometer (VSM). The hydrophilicity of the nanocomposites was revealed with contact angle analyzer JY-82B (Dingsheng, China). Zeta potential of the nanocomposites was measured by Brookhaven ZETAPALS/BI-200SM (USA) at room temperature. Thermogravimetric analysis (TGA) was carried out in nitrogen atmosphere at a heating rate of  $10^\circ\text{C}\cdot\text{min}^{-1}$  from room temperature to  $800^\circ\text{C}$  (NETZCHSTA 449 F3, Germany). Matrix assisted laser desorption/ionization time-of-flight mass spectrometry (MALDI-TOF MS) were performed on a Bruker Auto flex III LRF200-CID instrument (Bruker Daltonics, Germany) with a pulsed nitrogen laser operating at 337 nm in linear positive ion mode and DHB (25  $\text{mg}\cdot\text{mL}^{-1}$ ,  $\text{ACN}/\text{H}_2\text{O}/\text{TFA}$ , 80:19:1, v/v/v) was used as matrix.

**Preparation of  $\text{Fe}_3\text{O}_4$ -GO nanocomposites.**  $\text{Fe}_3\text{O}_4$ -GO NPs were synthesized with a solvothermal-method<sup>29</sup>. Typically, GO (48.7 mg), NaAc (1.36 g) and  $\text{FeCl}_3 \cdot 6\text{H}_2\text{O}$  (152 mg) were dissolved in EG (30 mL) under sonication for 2 h. The homogeneous solution was poured into a Teflon-lined stainless-steel autoclave (50 mL) and maintained at  $180^\circ\text{C}$  for 16 h. With the help of an external magnetic field, the prepared  $\text{Fe}_3\text{O}_4$ -GO nanocomposites were separated from the reaction solvent and washed with deionized water and ethanol for several times, and dried in vacuum at  $40^\circ\text{C}$  for 3 h.

**Preparation of  $\text{Fe}_3\text{O}_4$ -GO@PDA nanocomposites.** The  $\text{Fe}_3\text{O}_4$ -GO nanocomposites (40 mg) were dispersed in Tris buffer (100 mL, 10 mM, pH 8.5) under sonication, and dopamine chloride (30 mg) was added to the above solution. The mixture was stirred mechanically at  $60^\circ\text{C}$  for 24 h. In an external magnetic field, the prepared  $\text{Fe}_3\text{O}_4$ -GO@PDA nanocomposites were separated from the reaction solvent and washed with deionized water and ethanol for several times, and dried in vacuum at  $40^\circ\text{C}$  for 3 h.

**Degradation of chitosan by hydrogen peroxide.** 5%  $\text{H}_2\text{O}_2$  (100 mL) was added dropwise into the solution of Chitosan (10 g) in 2% acetic acid (200 mL). The mixture was stirred magnetically at  $60^\circ\text{C}$  for 8 h. Then the reaction solution was cooled and passed through two layers of filter paper. The aqueous phase obtained was retained and the pH was adjusted to 10.0 with 1 N NaOH, set aside for 2 h, and again filtrated through two layers of filter paper. After concentration under reduced pressure, the solution was diluted with methanol, set aside for 5 h. The white precipitation was collected via filtration and washed with methanol. The white powder was obtained after drying under vacuum.

**Preparation of  $\text{Fe}_3\text{O}_4$ -GO@PDA-Chitosan nanocomposites.** Into the solution of chitosan (120 mg) in Tris-HCl buffer (120 mL, pH 8.5), the  $\text{Fe}_3\text{O}_4$ -GO@PDA-Chitosan nanocomposites (30 mg) was dispersed under sonication. The mixture was stirred mechanically at room temperature for 24 h. In an external magnetic field, the prepared  $\text{Fe}_3\text{O}_4$ -GO@PDA-Chitosan nanocomposites were separated from the reaction solvent and washed with deionized water and ethanol for several times, and dried in vacuum at  $40^\circ\text{C}$  for 3 h.

**Digestion of proteins.** 1 mg HRP (human IgG or BSA) was dissolved in 1 mL  $\text{NH}_4\text{HCO}_3$  solution (50 mM, pH 8.3) under sonication and denatured by boiling for 15 min in water bath. And then, the denatured proteins were reduced with 3.1 mg DTT at  $37^\circ\text{C}$  for 2 h in water bath and alkylated by 7.2 mg IAA using a shaking table at room temperature in the dark for 40 min. The mixture was incubated with trypsin at an enzyme-protein ratio of 1:25 (w/w) at  $37^\circ\text{C}$  for 16 h. The tryptic digests were stored at  $-20^\circ\text{C}$  for later use.

Proteins extracted from human renal mesangial cells (HRMC) were precipitated by trichloroacetic acid and collected by centrifugation. The pellet was dissolved in 100 mM of  $\text{NH}_4\text{HCO}_3$ . The proteins underwent reduction, alkylation, and enzymolysis in sequence. The resulting digests were desalted using Sep-pak C18 cartridges (Water Ltd., Elstree, UK), evaporated to dryness, and stored at  $-20^\circ\text{C}$  for later use.

**N-Glycopeptides enrichment under hydrophilic mode.**  $\text{Fe}_3\text{O}_4$ -GO@PDA-Chitosan nanocomposites (or  $\text{Fe}_3\text{O}_4$ -GO@PDA, 40  $\mu\text{g}$ ) were rinsed thrice with the loading buffer ( $\text{ACN}/\text{H}_2\text{O}/\text{TFA} = 89:10.5:0.5$ , v/v/v), and then dispersed via ultrasonication in the above buffer (400  $\mu\text{L}$ ) containing a determined amount of HRP or IgG digests. After incubation at room temperature for 30 min, the nanocomposites were then washed thrice with the loading buffer. Finally, the N-glycopeptides captured by the  $\text{Fe}_3\text{O}_4$ -GO@PDA-Chitosan nanocomposites (or  $\text{Fe}_3\text{O}_4$ -GO@PDA) were released by  $2 \times 13 \mu\text{L}$  elution buffer ( $\text{ACN}/\text{H}_2\text{O}/\text{TFA} = 30:69.9:0.1$ , v/v/v). The supernatant was collected, lyophilized, re-dissolved in 4  $\mu\text{L}$  elution buffer and analyzed by MALDI-TOF MS.

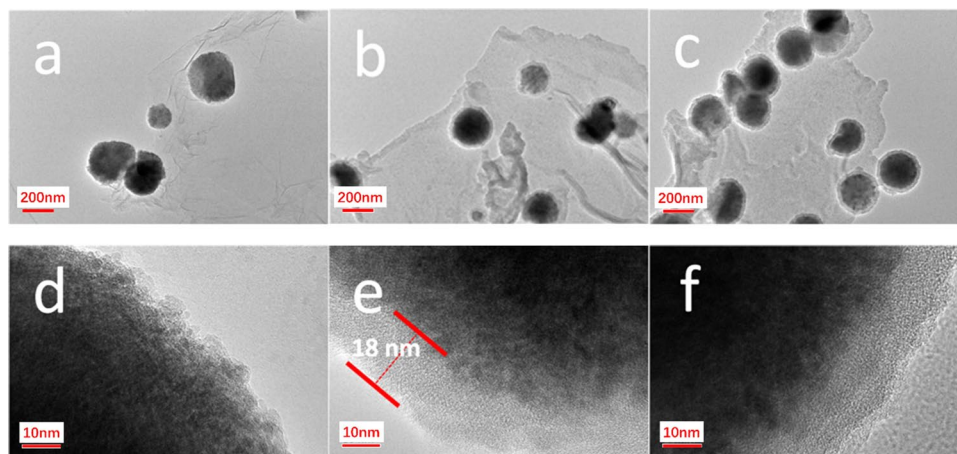


**Figure 2.** TEM images of  $\text{Fe}_3\text{O}_4$ -GO (a,d),  $\text{Fe}_3\text{O}_4$ -GO@PDA (b,e) and  $\text{Fe}_3\text{O}_4$ -GO@PDA-Chitosan (c,f) nanocomposites.

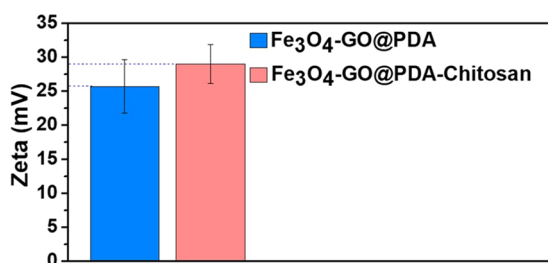


**Figure 3.** Zeta potential of  $\text{Fe}_3\text{O}_4$ -GO@PDA and  $\text{Fe}_3\text{O}_4$ -GO@PDA-Chitosan nanocomposites.

For the enrichment of N-glycopeptides from digests of human renal mesangial cells (HRMC, kindly donated by Dr. Mingzhen Li (Metabolic Diseases Hospital, Tianjin Medical University, Tianjin, China)), the operation was carried out according to a previous report<sup>30</sup>. Briefly, 200  $\mu\text{g}$  of the sample was dissolved in 5 mL of loading buffer (ACN/ $\text{H}_2\text{O}$ /TFA = 89:10.5:0.5, v/v/v), incubated with 20 mg of  $\text{Fe}_3\text{O}_4$ -GO@PDA-Chitosan nanocomposites for 1 h, and washed thrice with 2 mL of loading buffer. Then, the trapped glycopeptides were eluted twice with 400  $\mu\text{L}$  of elution buffer, and the elution was evaporated to dryness. The obtained glycopeptides were redissolved in 10 mM of  $\text{NH}_4\text{HCO}_3$ , and glycan moieties were removed by 1000 unites of PNGase F. The mixture was desalted and enriched using Sep-pak C18 cartridges (Waters Ltd., Elstree, UK), evaporated to dryness, and redissolved prior to analysis by nano LC-MS/MS.

## Results and Discussion

**Preparation and characterization of  $\text{Fe}_3\text{O}_4$ -GO@PDA-Chitosan nanocomposites.** The morphology of  $\text{Fe}_3\text{O}_4$ -GO,  $\text{Fe}_3\text{O}_4$ -GO@PDA,  $\text{Fe}_3\text{O}_4$ -GO@PDA-Chitosan nanocomposites and the thickness of the grafted PDA layer were revealed by transmission electron microscopy (TEM) at the 200 or 10 nanometer scale. As shown in Fig. 2a,d,  $\text{Fe}_3\text{O}_4$  nanoparticles were irregularly interspersed on the graphene nanosheets, indicating the successful assembly of  $\text{Fe}_3\text{O}_4$ -GO nanocomposites. By means of self-polymerization, the PDA layer was coated on the surface of  $\text{Fe}_3\text{O}_4$ -GO with the thickness of  $\sim 18$  nm (Fig. 2b,e). The molecular weight of degraded chitosan was determined to be  $\sim 1471$  g $\cdot\text{mol}^{-1}$  by Gel Permeation Chromatography, so the modification of degraded chitosan on the surface of  $\text{Fe}_3\text{O}_4$ -GO@PDA nanocomposites was not detected. When the chitosan shell was formed on the surface of  $\text{Fe}_3\text{O}_4$ -GO@PDA, the obtained  $\text{Fe}_3\text{O}_4$ -GO@PDA-Chitosan displayed an obvious core-shell structure (Fig. 2c,f).

The Zeta potentials of the obtained nanocomposites were detected in acid aqueous solution ( $\text{H}_2\text{O}$ /TFA = 99.5:0.5, v/v). The zeta potential of  $\text{Fe}_3\text{O}_4$ -GO@PDA was 25.70 mV (Fig. 3), which indicated that there were abundant phenolic group and amino groups onto the surface of PDA layer. And after graft of chitosan on the surface of PDA layer, the zeta potential increased to 29.01 mV due to the addition of amine and hydroxyl groups.

The magnetic properties of the obtained nanocomposites were measured by a vibrating sample magnetometer (VSM) at room temperature. The saturation magnetic ( $M_s$ ) values of  $\text{Fe}_3\text{O}_4$ -GO,  $\text{Fe}_3\text{O}_4$ -GO@PDA and  $\text{Fe}_3\text{O}_4$ -GO@PDA-Chitosan nanocomposites were 34.06, 19.66, 16.21 emu $\cdot\text{g}^{-1}$ , respectively (Fig. S1, Electronical Supporting Materials). Although the saturation magnetization value of  $\text{Fe}_3\text{O}_4$ -GO@PDA-Chitosan was reduced to 16.21 emu $\cdot\text{g}^{-1}$ , the  $\text{Fe}_3\text{O}_4$ -GO@PDA-Chitosan nanocomposites can be quickly separated within 10 s under an external magnetic field (Fig. S1 inset, Electronical Supporting Materials) and re-dispersed quickly after removal of the magnetic field.

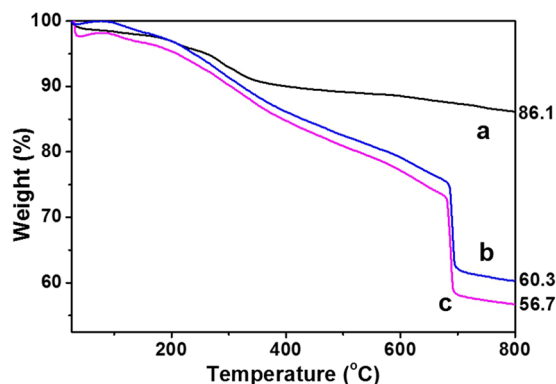


**Figure 4.** TGA curves of  $\text{Fe}_3\text{O}_4$  (a),  $\text{Fe}_3\text{O}_4\text{-GO@PDA}$  (b) and  $\text{Fe}_3\text{O}_4\text{-GO@PDA-Chitosan}$  (c) nanocomposites.

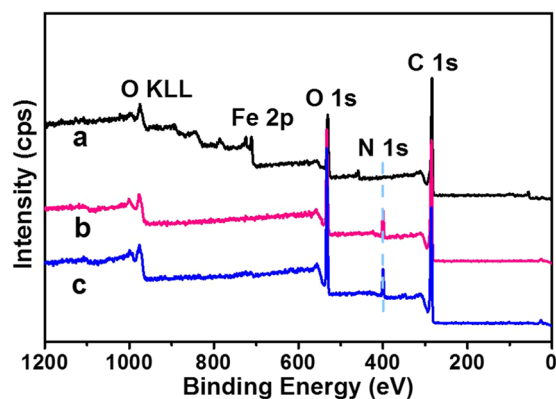


**Figure 5.** XPS spectrum of  $\text{Fe}_3\text{O}_4$  (a),  $\text{Fe}_3\text{O}_4\text{-GO@PDA}$  (b) and  $\text{Fe}_3\text{O}_4\text{-GO@PDA-Chitosan}$  (c) nanocomposites.

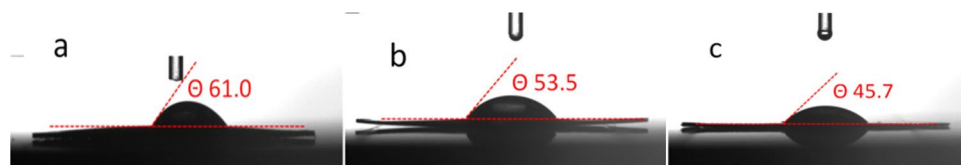


**Figure 6.** Water contact angles of  $\text{Fe}_3\text{O}_4$  (a),  $\text{Fe}_3\text{O}_4\text{-GO@PDA}$  (b) and  $\text{Fe}_3\text{O}_4\text{-GO@PDA-Chitosan}$  (c) nanocomposites.

The crystalline phases of  $\text{Fe}_3\text{O}_4\text{-GO}$ ,  $\text{Fe}_3\text{O}_4\text{-GO@PDA}$  and  $\text{Fe}_3\text{O}_4\text{-GO@PDA-Chitosan}$  nanocomposites were characterized by the XRD technique (Fig. S2, Electronical Supporting Materials). Six discernible diffraction peaks at  $30.06^\circ$ ,  $35.36^\circ$ ,  $43.16^\circ$ ,  $53.42^\circ$ ,  $57.08^\circ$ ,  $62.50^\circ$  were indexed as (220), (311), (400), (422), (511) and (440) in the database of the Joint Committee on Powder Diffraction Standards (JCPDS card: 19-0629). This result indicated that the presence of  $\text{Fe}_3\text{O}_4$  nanoparticles in the nanocomposites.

The thermogravimetric analysis (TGA) curves of  $\text{Fe}_3\text{O}_4\text{-GO}$ ,  $\text{Fe}_3\text{O}_4\text{-GO@PDA}$  and  $\text{Fe}_3\text{O}_4\text{-GO@PDA-Chitosan}$  nanocomposites are shown in Fig. 4. It can be found that 13.9% weight loss occurred for  $\text{Fe}_3\text{O}_4\text{-GO}$  (Fig. 4a) corresponding to the content of GO. And there were 39.7 and 43.3% weight loss for  $\text{Fe}_3\text{O}_4\text{-GO@PDA}$  (Fig. 4b) and  $\text{Fe}_3\text{O}_4\text{-GO@PDA-Chitosan}$  (Fig. 4c), respectively. From the data of TGA curves, the amount of immobilized chitosan onto the  $\text{Fe}_3\text{O}_4\text{-GO@PDA-Chitosan}$  nanocomposites was calculated to  $24.5 \mu\text{mol}\cdot\text{g}^{-1}$ .

The surface composition of the obtained nanocomposites ( $\text{Fe}_3\text{O}_4\text{-GO}$ ,  $\text{Fe}_3\text{O}_4\text{-GO@PDA}$ ,  $\text{Fe}_3\text{O}_4\text{-GO@PDA-Chitosan}$ ) were characterized by XPS. As shown in Fig. 5, the peaks of Fe 2p, O 1s, N 1s and C 1s were evidently observed. The contact angle of prepared nanocomposites ( $\text{Fe}_3\text{O}_4\text{-GO}$ ,  $\text{Fe}_3\text{O}_4\text{-GO@PDA}$ ,  $\text{Fe}_3\text{O}_4\text{-GO@PDA-Chitosan}$ ) were measured with the powder tableting method (Fig. 6) to evaluate the relative surface hydrophilicity. The contact angle of  $\text{Fe}_3\text{O}_4\text{-GO}$  (a),  $\text{Fe}_3\text{O}_4\text{-GO@PDA}$  (b) and  $\text{Fe}_3\text{O}_4\text{-GO@PDA-Chitosan}$  (c) nanocomposites were  $61.0^\circ$ ,  $53.5^\circ$ , and  $45.7^\circ$ , respectively. It indicated that the polydopamine layer coated on the surface of magnetic graphene played a role not only in facile synthesis procedure via Michael addition, but also in hydrophilicity raise; the modification of chitosan improved further the hydrophilicity of the nanocomposites.

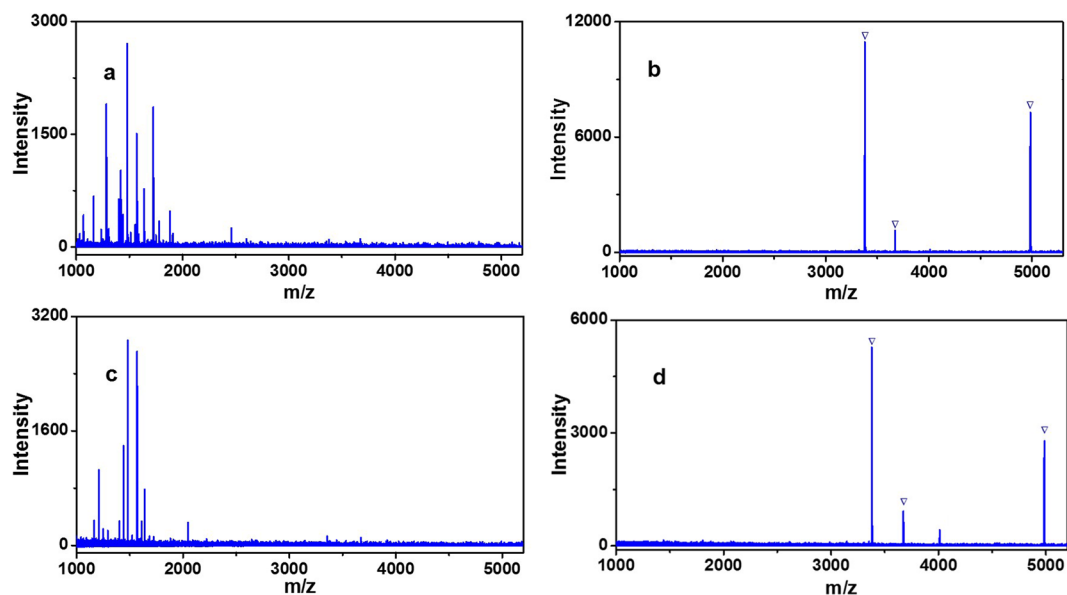


**Figure 7.** MALDI-TOF mass analysis of tryptic digest of HRP ( $50 \text{ fmol} \cdot \mu\text{L}^{-1}$ ): (a) before enrichment, (b) eluent and (c) supernatant after enrichment with  $\text{Fe}_3\text{O}_4\text{-GO@PDA-Chitosan}$  nanocomposites; eluent after enrichment with (d)  $\text{Fe}_3\text{O}_4\text{-GO@PDA}$  nanocomposites. The peaks of glycopeptides are marked with  $\nabla$ .

### Glycopeptide enrichment from standard proteins by $\text{Fe}_3\text{O}_4\text{-GO@PDA-Chitosan}$ nanocomposites.

To select the optimal enrichment condition to glycopeptides, three different kinds of loading buffer (89% ACN/ $\text{H}_2\text{O}$ , 0.1% TFA; 89% ACN/ $\text{H}_2\text{O}$ , 0.5% TFA; 89% ACN/ $\text{H}_2\text{O}$ , 1% TFA) were utilized for investigate the effect of capturing glycopeptides from HRP digestion by  $\text{Fe}_3\text{O}_4\text{-GO@PDA-Chitosan}$  nanocomposites and the results were displayed in Fig. S3 (Electronical Supporting Materials). The performance of  $\text{Fe}_3\text{O}_4\text{-GO@PDA-Chitosan}$  nanocomposites for enrichment of N-glycopeptides was the best in the loading buffer (89% ACN/ $\text{H}_2\text{O}$ , 0.5% TFA). By taking advantage of the optimized enrichment condition,  $\text{Fe}_3\text{O}_4\text{-GO@PDA-Chitosan}$  nanocomposites were applied to capture N-glycopeptides from standard HRP tryptic digest ( $50 \text{ fmol} \cdot \mu\text{L}^{-1}$ ). As shown in Fig. 7a, the direct analysis of HRP digest ( $50 \text{ fmol} \cdot \mu\text{L}^{-1}$ ) without enrichment step, the signal peaks of low abundance of N-glycopeptides were completely suppressed, no target analyte was detected. After enrichment by  $\text{Fe}_3\text{O}_4\text{-GO@PDA-Chitosan}$  nanocomposites, the number and signal intensity of glycopeptides were distinctly enhanced, meanwhile, three N-glycopeptides were detected and non-glycopeptides were completely removed (Fig. 7b, detailed information is listed in Table S1, Electronical Supporting Materials). And no glycopeptides peaks were found in the supernatant (Fig. 7c). For comparison, three N-glycopeptides were also identified after enrichment with  $\text{Fe}_3\text{O}_4\text{-GO@PDA}$  nanocomposites, but the signal intensity was weaker and the one signal peak of non-glycopeptide appeared in MS spectra (Fig. 7d).

The detection sensitivity of  $\text{Fe}_3\text{O}_4\text{-GO@PDA-Chitosan}$  (or  $\text{Fe}_3\text{O}_4\text{-GO@PDA}$ ) nanocomposites for N-glycopeptides enrichment was evaluated with lower concentrations of HRP tryptic digests. When the concentration of HRP digestion decreased to  $0.5 \text{ fmol} \cdot \mu\text{L}^{-1}$ , five N-glycopeptides were detected after enrichment with  $\text{Fe}_3\text{O}_4\text{-GO@PDA-Chitosan}$  nanocomposites, and four N-glycopeptides and one non-glycopeptide were detected after enrichment with  $\text{Fe}_3\text{O}_4\text{-GO@PDA}$  nanocomposites (Fig. 8a,b). Even at the concentration of  $0.4 \text{ fmol} \cdot \mu\text{L}^{-1}$ , two N-glycopeptides were still observed after treatment of  $\text{Fe}_3\text{O}_4\text{-GO@PDA-Chitosan}$  nanocomposites (Fig. 8c). The detection sensitivity of  $\text{Fe}_3\text{O}_4\text{-GO@PDA-Chitosan}$  nanocomposites was higher than some reported hydrophilic nanomaterials, such as Au NP-maltose/PDA/ $\text{Fe}_3\text{O}_4\text{-RGO}$  ( $2.5 \text{ fmol} \cdot \mu\text{L}^{-1}$ )<sup>29</sup>,  $\text{Fe}_3\text{O}_4\text{-DA-Maltose}$  ( $1.25 \text{ fmol} \cdot \mu\text{L}^{-1}$ )<sup>31</sup>,  $\text{Fe}_3\text{O}_4\text{@mSiO}_2\text{@G6P}$  ( $0.5 \text{ fmol} \cdot \mu\text{L}^{-1}$ )<sup>32</sup>, mMOF@Au@GSH ( $0.5 \text{ fmol} \cdot \mu\text{L}^{-1}$ )<sup>20</sup>.

The enrichment selectivity of  $\text{Fe}_3\text{O}_4\text{-GO@PDA-Chitosan}$  nanocomposites was further investigated, by evaluating the capture performance for N-glycopeptides from the mixture of HRP and BSA tryptic digest with different molar ratios. When the molar ratio of digests mixture of HRP and BSA was 1:1 or 1:10, the MS signals of N-glycopeptides were completely suppressed in direct analysis due to the strong signal suppression from an amount of non-glycopeptides (Fig. 9a,c). By contrast, after enrichment by  $\text{Fe}_3\text{O}_4\text{-GO@PDA-Chitosan}$  nanocomposites, two N-glycopeptides derived from HRP were detected with no non-glycopeptide signals (Fig. 9b). The molar ratio of HRP and BSA was further increased even 1:10, an overwhelming majority of non-glycopeptides were removed and the peaks of N-glycopeptides still absolutely dominated MS spectra (Fig. 9d). The enrichment selectivity of  $\text{Fe}_3\text{O}_4\text{-GO@PDA-Chitosan}$  nanocomposites was higher than some reported hydrophilic nanomaterials functionalized with saccharides, such as Au NP-maltose/PDA/ $\text{Fe}_3\text{O}_4\text{-RGO}$ <sup>29</sup>,  $\text{Fe}_3\text{O}_4\text{-DA-Maltose}$ <sup>31</sup>, MagG/Au/Glu<sup>33</sup>. The results indicated that  $\text{Fe}_3\text{O}_4\text{-GO@PDA-Chitosan}$  nanocomposites have the great potential in N-glycopeptides enrichment from complex biological sample.

To demonstrate the unbiased enrichment performance of  $\text{Fe}_3\text{O}_4\text{-GO@PDA-Chitosan}$  nanocomposites towards different N-glycan, it was applied to capture N-glycopeptides from IgG digest, which contains different glycoforms from HRP. In direct MS analysis without enrichment, no N-glycopeptides were detected on account

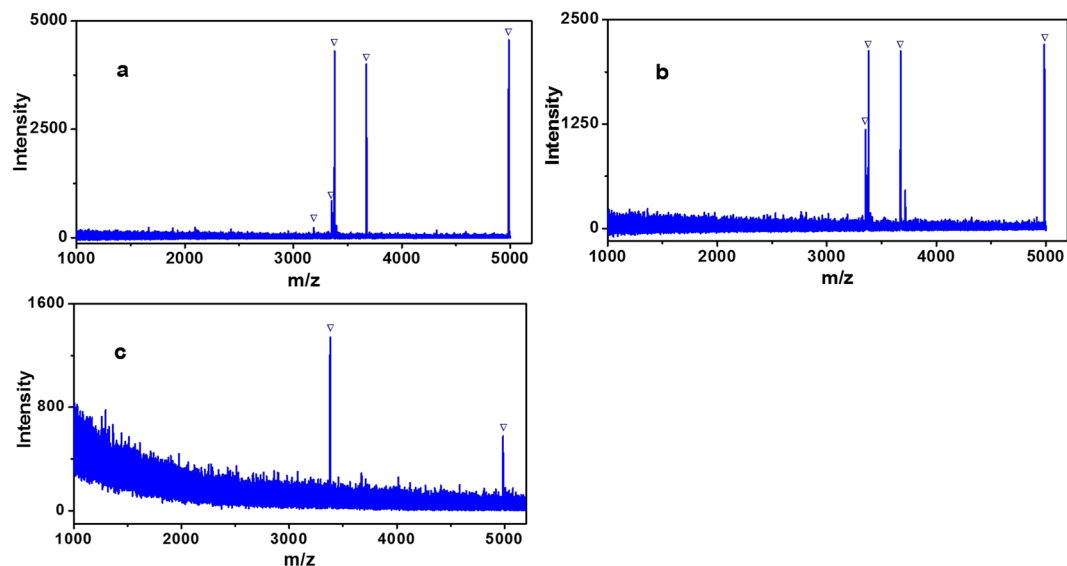


**Figure 8.** MALDI-TOF mass analysis of tryptic digest of HRP ( $0.5 \text{ fmol} \cdot \mu\text{L}^{-1}$ ) after enrichment with  $\text{Fe}_3\text{O}_4\text{-GO@PDA-Chitosan}$  (a) and  $\text{Fe}_3\text{O}_4\text{-GO@PDA}$  nanocomposites (b); MALDI-TOF mass analysis of tryptic digest of HRP ( $0.4 \text{ fmol} \cdot \mu\text{L}^{-1}$ ) after enrichment with  $\text{Fe}_3\text{O}_4\text{-GO@PDA-Chitosan}$  (c) nanocomposites. The peaks of glycopeptides are marked with  $\nabla$ .

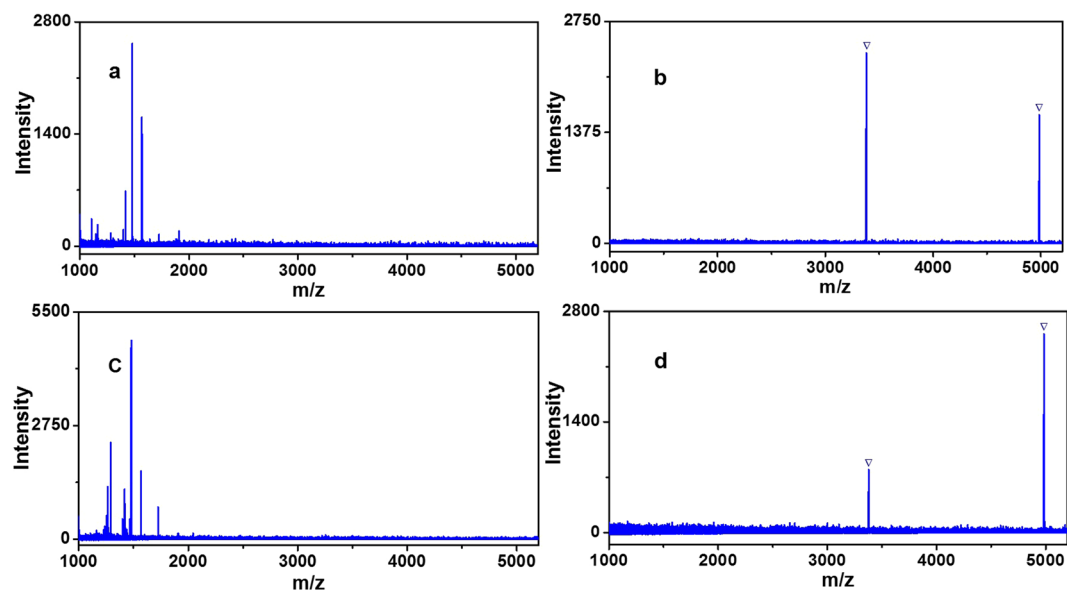


**Figure 9.** MALDI-TOF mass spectra of mixture of tryptic HRP and BSA before enrichment: (a) 1:1; (c) 1:10. MALDI-TOF MS spectra of the identified glycopeptides enriched by  $\text{Fe}_3\text{O}_4\text{-GO@PDA-Chitosan}$  nanocomposites from the tryptic mixture of HRP and BSA with the molar ratio of (b) 1:1; (d) 1:10. The peaks of glycopeptides are marked with  $\nabla$ .

of the strong interference from non-glycopeptides (Fig. 10a). Seven N-glycopeptides were identified after enrichment with  $\text{Fe}_3\text{O}_4\text{-GO@PDA}$  nanocomposites (Fig. 10b). For comparison, fifteen N-glycopeptides were detected after enrichment by  $\text{Fe}_3\text{O}_4\text{-GO@PDA-Chitosan}$  nanocomposites (Fig. 10c, detailed information is listed in Table S2, Electronical Supporting Materials), and the signal intensity was stronger in MS spectra. The eluted glycopeptides from  $\text{Fe}_3\text{O}_4\text{-GO@PDA-Chitosan}$  nanocomposites enrichment were deglycosylated by PNGase F and two strong signals of deamidated peptides (at  $m/z$  1158.4 (EEQFN#STFR), 1190.4 (EEQYN#STFR)) were detected (Fig. 10d), which demonstrated that the enriched peptide fragments were N-glycopeptides.

**Evaluation of binding capacity of  $\text{Fe}_3\text{O}_4\text{-GO@PDA-Chitosan}$  nanocomposites for N-glycopeptide enrichment.** Different masses ( $20\text{-}100 \mu\text{g}$ ) of  $\text{Fe}_3\text{O}_4\text{-GO@PDA-Chitosan}$  nanocomposites

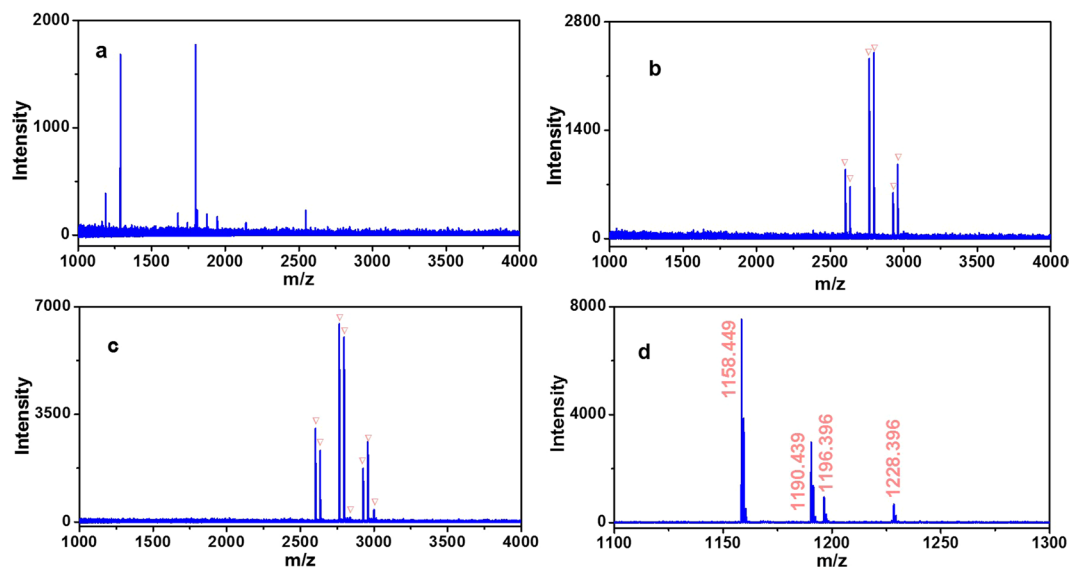


**Figure 10.** MALDI-TOF mass spectra of tryptic digests of IgG ( $5 \text{ fmol} \cdot \mu\text{L}^{-1}$ ): direct analysis (a); analysis after enrichment with  $\text{Fe}_3\text{O}_4\text{-GO@PDA}$  (b) or  $\text{Fe}_3\text{O}_4\text{-GO@PDA-Chitosan}$  nanocomposites (c), and deglycosylation by PNGase F (d). The peaks of glycopeptides are marked with  $\nabla$ .

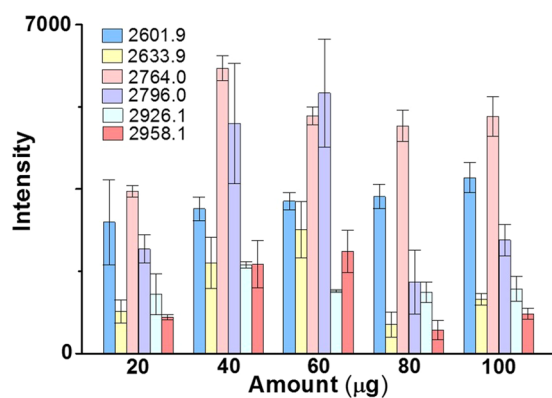


**Figure 11.** The intensity of six selected N-glycopeptides from tryptic digests of human IgG ( $3 \mu\text{g}$ ) after enrichment by different amount of  $\text{Fe}_3\text{O}_4\text{-GO@PDA-Chitosan}$  nanocomposites.

were dispersed with ultrasonication for 6 s in the loading buffer ( $400 \mu\text{L}$ ,  $V(\text{ACN})/V(\text{H}_2\text{O})/V(\text{TFA}) = 89:10.5:0.5$ ) containing human IgG digest ( $3 \mu\text{g}$ ). After the enrichment, the elution was analyzed with MALDI-TOF MS. When the MS signal intensity of six selected glycopeptides reach maximum, the total amount of glycopeptides were captured by the nanocomposites. The binding capacity was calculated by the mass ratio of human IgG ( $3 \mu\text{g}$ ) and the  $\text{Fe}_3\text{O}_4\text{-GO@PDA-Chitosan}$  nanocomposites. As shown in Fig. 11, the N-glycopeptides from human IgG digest ( $3 \mu\text{g}$ ) were almost bonded onto  $40 \mu\text{g}$  of  $\text{Fe}_3\text{O}_4\text{-GO@PDA-Chitosan}$  nanocomposites, and the binding capacity of the nanocomposites was about  $75 \text{ mg} \cdot \text{g}^{-1}$ , Which was higher than some reported hydrophilic materials modified with saccharides such as  $\text{Fe}_3\text{O}_4\text{@CS MCNCs}$  ( $17.5 \text{ mg} \cdot \text{g}^{-1}$ )<sup>25</sup> and  $\text{Fe}_3\text{O}_4\text{-DA-Maltose}$  ( $43 \text{ mg} \cdot \text{g}^{-1}$ )<sup>31</sup>. Meanwhile, the binding capacity of  $\text{Fe}_3\text{O}_4\text{-GO@PDA}$  nanocomposites was evaluated, the N-glycopeptides from human IgG digest ( $3 \mu\text{g}$ ) were almost bonded onto  $80 \mu\text{g}$  of  $\text{Fe}_3\text{O}_4\text{-GO@PDA}$  nanocomposites, and the binding capacity of the nanocomposites was about  $37.5 \text{ mg} \cdot \text{g}^{-1}$  (Fig. S4, Electronical Supporting Materials).

**The stability and reusability of  $\text{Fe}_3\text{O}_4\text{-GO@PDA-Chitosan}$  nanocomposites.** To evaluate the stability and reusability of  $\text{Fe}_3\text{O}_4\text{-GO@PDA-Chitosan}$  nanocomposites, the material was firstly placed in a glass vial for three months at room temperature, and then applied to capture N-glycopeptides from HRP digest for four cycles. As shown in Fig. S5 (Electronical Supporting Materials), the enrichment performance of  $\text{Fe}_3\text{O}_4\text{-GO@PDA-Chitosan}$  nanocomposites in the first time and fourth time was all good, which indicates that the  $\text{Fe}_3\text{O}_4\text{-GO@PDA-Chitosan}$  nanocomposites own good stability and repeatability.

**Practical application of  $\text{Fe}_3\text{O}_4\text{-GO@PDA-Chitosan}$  nanocomposites on glycopeptide enrichment.** In order to test the practical application of  $\text{Fe}_3\text{O}_4\text{-GO@PDA-Chitosan}$  nanocomposites on glycopeptide



enrichment in the complex samples, the Fe<sub>3</sub>O<sub>4</sub>-GO@PDA-Chitosan nanocomposites were applied to analyze the N-linked glycopeptides from the human renal mesangial cells (HRMC). HRMC serve as a filtration barrier of the kidney. The injury of mesangial cells could cause diabetic nephropathy, leading end-stage renal disease. Emerging evidence indicates that mesangial cells can be damaged by high glucose, however the mechanism is unclear. In this work, Fe<sub>3</sub>O<sub>4</sub>-GO@PDA-Chitosan nanocomposites were used to enrich the N-link glycopeptide from the HRMC which have been treated by high glucose and the glycopeptide enrichment was further identified by HPLC-MS/MS (The details of cell culture, protein extraction and MS/MS data analysis in the Electrical Supporting Materials). Finally, 393 N-linked glycopeptides, representing 195 different glycoproteins and 458 glycosylation sites were identified in HRMC (Table S3, Electrical Supporting Materials).

## Conclusion

In summary, the novel chitosan-interspersed magnetic nanocomposites (Fe<sub>3</sub>O<sub>4</sub>-GO@PDA-Chitosan) were prepared successfully via a facile two-step method for selective enrichment of N-glycopeptides. Due to the enhanced hydrophilicity by the PDA layer and chitosan, the resulting nanocomposites exhibited good selectivity and sensitivity for N-glycopeptides enrichment from the complex biological samples. The combination of dopamine self-polymerization and Michael addition is a feasible strategy to assemble hydrophilic nanomaterials applied in N-glycopeptides enrichment.

Received: 28 January 2019; Accepted: 30 September 2019;

Published online: 09 January 2020

## References

- Jürgen, R. Protein N-glycosylation along the secretory pathway: relationship to organelle topography and function, protein quality control, and cell interactions. *Chem. Rev.* **102**, 285–303 (2002).
- Hart, G. W. & Copeland, R. J. Glycomics hits the big time. *Cell* **143**, 672–676 (2010).
- Jürgen, R. *et al.* Protein N-glycosylation, protein folding, and protein quality control. *Mol. Cells* **30**, 497–506 (2010).
- Parekh, R. B. *et al.* Association of rheumatoid arthritis and primary osteoarthritis with changes in the glycosylation pattern of total serum IgG. *Nature* **316**, 452–457 (1985).
- Moran, F. P. *et al.* Interplay between protein glycosylation pathways in alzheimer's disease. *Sci. Adv.* **3**, e1601576 (2017).
- Green, R. S. *et al.* Mammalian N-glycan branching protects against innate immune self-recognition and inflammation in autoimmune disease pathogenesis. *Immunity* **27**, 308–320 (2007).
- Lan, Y. *et al.* Serum glycoprotein-derived N- and O-linked glycans as cancer biomarkers. *Am. J. Cancer Res.* **6**, 2390–2415 (2016).
- Alley, J. W. Jr., Mann, F. B. & Novotny, V. M. High-sensitivity analytical approaches for the structural characterization of glycoproteins. *Chem. Rev.* **113**, 2668–2732 (2013).
- Xiao, H. P., Chen, W. X., Smeekens, M. J. & Wu, R. H. An enrichment method based on synergistic and reversible covalent interactions for large-scale analysis of glycoproteins. *Nat. Commun.* **9**, 1692 (2018).
- Zhang, X. H., Wang, J. W., He, X. W., Chen, L. X. & Zhang, Y. K. Tailor-made boronic acid functionalized magnetic nanoparticles with a tunable polymer shell-assisted for the selective enrichment of glycoproteins/glycopeptides. *ACS Appl. Mater. Interfaces* **7**, 24576–24584 (2015).
- Wu, Q. *et al.* 3-Carboxybenzoboroxole functionalized polyethylenimine modified magnetic graphene oxide nanocomposites for human plasma glycoproteins enrichment under physiological conditions. *Anal. Chem.* **90**, 2671–2677 (2018).
- Liu, J. X. *et al.* Boronic acid-functionalized particles with flexible three-dimensional polymer branch for highly specific recognition of glycoproteins. *ACS Appl. Mater. Interfaces* **8**, 9552–9556 (2016).
- Tan, S. Y., Wang, J. D., Han, Q., Liang, Q. L. & Ding, M. Y. A porous graphene sorbent coated with titanium (IV)-functionalized polydopamine for selective lab-in-syringe extraction of phosphoproteins and phosphopeptides. *Microchim. Acta* **185**, 316 (2018).
- Zou, X. J., Jie, J. Z. & Yang, B. Single-step enrichment of N-glycopeptides and phosphopeptides with novel multifunctional Ti<sup>4+</sup>-immobilized dendritic polyglycerol coated chitosan nanomaterials. *Anal. Chem.* **89**, 7520–7526 (2017).
- Hong, Y. Y. *et al.* Hydrophilic phytic acid-coated magnetic graphene for titanium (IV) immobilization as a novel hydrophilic interaction liquid chromatography-immobilized metal affinity chromatography. *Anal. Chem.* **90**, 11008–11015 (2018).
- Bie, Z. J., Chen, Y., Ye, J., Wang, S. S. & Liu, Z. Boronate-affinity glycan-oriented surface imprinting: a new strategy to mimic lectins for the recognition of an intact glycoprotein and its characteristic fragments. *Angew. Chem. Int. Ed.* **54**, 10211–10215 (2015).
- Sun, X. Y., Ma, R.-T., Chen, J. & Shi, Y.-P. Magnetic boronate modified molecularly imprinted polymers on magnetite microspheres modified with porous TiO<sub>2</sub> (Fe<sub>3</sub>O<sub>4</sub>@pTiO<sub>2</sub>@MIP) with enhanced adsorption capacity for glycoproteins and with wide operational pH range. *Microchim. Acta* **185**, 565 (2018).
- Luo, J. *et al.* Double recognition and selective extraction of glycoprotein based on the molecular imprinted graphene oxide and boronate affinity. *ACS Appl. Mater. Interfaces* **9**, 7735–7744 (2017).
- Ma, W. *et al.* Cysteine-functionalized metal-organic framework: facile synthesis and high efficient enrichment of N-linked glycopeptides in cell lysate. *ACS Appl. Mater. Interfaces* **9**, 19562–19568 (2017).
- Liu, Q. J., Deng, C. H. & Sun, N. R. Hydrophilic tripeptide-functionalized magnetic metal-organic frameworks for the highly efficient enrichment of N-linked glycopeptides. *Nanoscale* **10**, 12149–12155 (2018).
- Xia, C. S. *et al.* Two-dimensional MoS<sub>2</sub>-based zwitterionic hydrophilic interaction liquid chromatography material for the specific enrichment of glycopeptides. *Anal. Chem.* **90**, 6651–6659 (2018).
- Sangram, K. S. *et al.* Cationic polymers and their therapeutic potential. *Chem. Soc. Rev.* **41**, 7147–7149 (2012).
- He, X. M. *et al.* High strength and hydrophilic chitosan microspheres for the selective enrichment of N-glycopeptides. *Anal. Chem.* **89**, 9712–9721 (2017).
- Li, Y. L., Wang, J. W., Sun, N. R. & Deng, C.-H. Glucose-6-phosphate-functionalized magnetic microspheres as novel hydrophilic probe for specific capture of N-linked glycopeptides. *Anal. Chem.* **89**, 11151–11158 (2017).
- Fang, C. L. *et al.* One-pot synthesis of magnetic colloidal nanocrystal clusters coated with chitosan for selective enrichment of glycopeptides. *Anal. Chim. Acta* **841**, 99–105 (2014).
- Wang, J. X., Li, J., Yan, G. Q., Gao, M. X. & Zhang, X. M. Preparation of a thickness-controlled Mg-MOFs-based magnetic graphene composite as a novel hydrophilic matrix for the effective identification of the glycopeptide in the human urine. *Nanoscale* **11**, 3701–3709 (2019).
- Jiang, B., Wu, Q., Zhang, L. H. & Zhang, Y. K. Preparation and application of silver nanoparticle-functionalized magnetic graphene oxide nanocomposites. *Nanoscale* **9**, 1607–1615 (2017).
- Wan, H. *et al.* A dendrimer-assisted magnetic graphene-silica hydrophilic composite for efficient and selective enrichment of glycopeptides from the complex sample. *Chem. Commun.* **51**, 9391–9394 (2015).

29. Bi, C. F., Jiang, R. D., He, X. W., Chen, L. X. & Zhang, Y. K. Synthesis of a hydrophilic maltose functionalized Au NP/PDA/Fe<sub>3</sub>O<sub>4</sub>-RGO magnetic nanocomposite for the highly specific enrichment of glycopeptides. *RSC Adv.* **5**, 59408–59416 (2015).
30. Bi, C. F. *et al.* Maltose-functionalized hydrophilic magnetic nanoparticles with polymer brushes for highly selective enrichment of N-linked glycopeptides. *ACS Omega* **3**, 1572–1580 (2018).
31. Bi, C. F. *et al.* Click synthesis of hydrophilic maltose-functionalized iron oxide magnetic nanoparticles based on dopamine anchors for highly selective enrichment of glycopeptides. *ACS Appl. Mater. Interfaces* **7**, 24670–24678 (2015).
32. Li, Y. L., Deng, C. H. & Sun, N. R. Hydrophilic probe in mesoporous pore for selective enrichment of endogenous glycopeptides in biological samples. *Anal. Chim. Acta* **1024**, 84–92 (2018).
33. Feng, X. Y., Deng, C. H., Gao, M. X., Yan, G. Q. & Zhang, X. M. Novel synthesis of glucose functionalized magnetic graphene hydrophilic nanocomposites via facile thiolation for high-efficient enrichment of glycopeptides. *Talanta* **179**, 377–385 (2018).

### Acknowledgements

We gratefully appreciate the financial support by the Natural Science Foundation of Tianjin City (No 18JCQNJC09500) and the CAMS Innovation Fund for Medical Sciences (CIFMS, 2017-I2M-3-019 and 2016-I2M-3-022).

### Author contributions

Langxing Chen and Changfen Bi conceived the experiments; Changfen Bi and Ye Yuan synthesized and characterized hydrophilic magnetic graphene nanocomposites, conducted the experiments and analyzed the results. Yuran Tu and Jiahui Wu completed the synthesis of degraded chitosan. YuLu Liang evaluated the stability and reusability of Fe<sub>3</sub>O<sub>4</sub>-GO@PDA-Chitosan nanocomposites. The manuscript was prepared by Changfen Bi, Langxing Chen, Yiliang Li, Xiwen He and Yukui Zhang. All authors edited the manuscript.

### Competing interests

The authors declare no competing interests.

### Additional information

**Supplementary information** is available for this paper at <https://doi.org/10.1038/s41598-019-56944-4>.

**Correspondence** and requests for materials should be addressed to Y.L. or L.C.

**Reprints and permissions information** is available at [www.nature.com/reprints](http://www.nature.com/reprints).

**Publisher's note** Springer Nature remains neutral with regard to jurisdictional claims in published maps and institutional affiliations.



**Open Access** This article is licensed under a Creative Commons Attribution 4.0 International License, which permits use, sharing, adaptation, distribution and reproduction in any medium or format, as long as you give appropriate credit to the original author(s) and the source, provide a link to the Creative Commons license, and indicate if changes were made. The images or other third party material in this article are included in the article's Creative Commons license, unless indicated otherwise in a credit line to the material. If material is not included in the article's Creative Commons license and your intended use is not permitted by statutory regulation or exceeds the permitted use, you will need to obtain permission directly from the copyright holder. To view a copy of this license, visit <http://creativecommons.org/licenses/by/4.0/>.

© The Author(s) 2020